A Letters Journal Exploring
the Frontiers of Physics

OFFPRINT

Branched Josephson junctions: Current carrying solitons in external magnetic fields

D. Matrasulov, K. Sabirov, D. Babajanov and H. Susanto

EPL, **130** (2020) 67002

A LETTERS JOURNAL EXPLORING
THE FRONTIERS OF PHYSICS

June 2020

EPL, **130** (2020) 67002
doi: 10.1209/0295-5075/130/67002

www.epljournal.org

Branched Josephson junctions: Current carrying solitons in external magnetic fields

D. MATRASULOV[1,2], K. SABIROV[3], D. BABAJANOV[1] and H. SUSANTO[4,5]

[1] *Turin Polytechnic University in Tashkent - 17 Niyazov Str., 100095, Tashkent, Uzbekistan*
[2] *Center for Nanotechnology, National University of Uzbekistan - 100174, Tashkent, Uzbekistan*
[3] *Tashkent University of Information Technology - Amir Temur Avenue 108, Tashkent 100200, Uzbekistan*
[4] *Department of Mathematical Sciences, University of Essex - Wivenhoe Park, Colchester CO4 3SQ, UK*
[5] *Department of Mathematics, Khalifa University, Abu Dhabi Campus - PO Box 127788, Abu Dhabi, United Arab Emirates*

received 18 October 2019; accepted in final form 17 June 2020
published online 6 July 2020

PACS 74.50.+r – Tunneling phenomena; Josephson effects
PACS 05.45.Yv – Solitons

Abstract – We consider the branched Josephson junction created by planar superconductors connected to each other through the Y-junction insulator. Assuming that the structure interacts with the external constant magnetic field, we study static sine-Gordon solitons in such system by modeling them in terms of the stationary sine-Gordon equation on metric graph. Exact analytical solutions of the problem are obtained and their stability is analyzed.

Introduction. – Low-dimensional nanoscale materials are the basic structures for many electronic devices. Optimization of their electronic properties and effective functioning of such devices require tuning the material properties and revealing the most appropriate device architecture. This concerns also superconducting structures such as Josephson junctions. A remarkable feature of Josephson junctions is the fact that the phase difference at the junction is described in terms of the sine-Gordon equation (see, *e.g.*, [1–8]). This makes them powerful testing ground for experimental realization of sine-Gordon solitons [9–15]. So far, different models have been proposed for the study of static and traveling solitons using Josephson junctions [16–33].

In this paper we address the problem of static solitons in branched Josephson junction containing planar superconductors connected to each other via the branched insulators having the shape of a Y-junction. The system is considered as interacting with constant external magnetic field. The phase differences on each branch of such structure is described in terms of the stationary sine-Gordon equation on metric graphs. Earlier, in ref. [34] we considered a version of such system for the case of absence of current-carrying states. Unlike that case, in the present study, including current leads to completely different vertex boundary conditions, and hence, to different solutions than those obtained in [34]. Provided certain constraints given in terms of the system parameters, we obtain exact analytical solutions of the stationary sine-Gordon equation on metric graphs, modeling static solitons in the branched Josephson junction. The motivation for the study of such model comes from several practically important problems, such as superconducting quantum interference devices (SQUID in networks), superconducting qubits in networks, as well as granular superconductors. Among others, the most attractive practical application could be experimental realization of sine-Gordon solitons in networks. We note that the soliton dynamics in networks is becoming one of the hot topics in nonlinear and mathematical physics [26,27,34–53]. References [26,27] considered for the first time the sine-Gordon equation on branched domain modeling of the Josephson junction at tricrystal surfaces. The integrable sine-Gordon equation on metric graphs is studied in [34,40,45]. Linear and nonlinear systems of PDE on metric graphs are considered in [48–50].

Among different realizations of Josephson junctions that having the discrete and branched structure is of special importance, as it allows to study soliton dynamics in discrete systems and networks. The early treatment of superconductor networks consisting of Josephson junctions meeting at one point dates back to [24]. An interesting realization of the Josephson junction networks at tricrystal boundaries was discussed earlier in [25], which inspired later

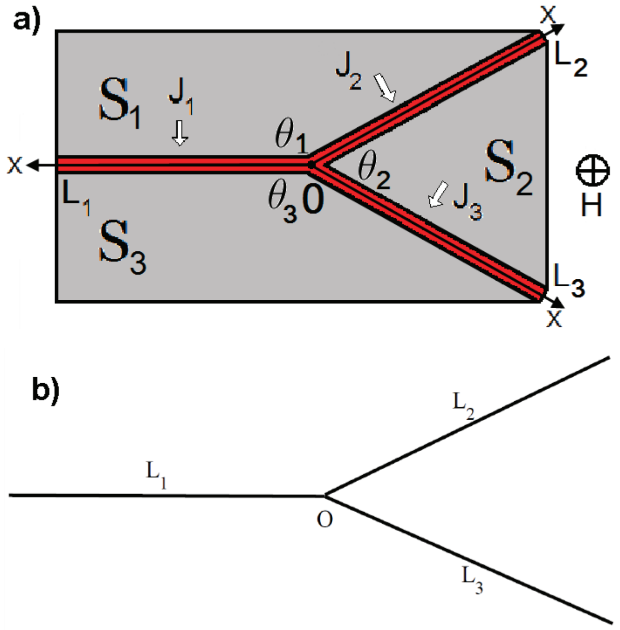

Fig. 1: (a) Branched Josephson Y-junction in a constant magnetic field, H. Red lines imply normal metal or insulator. J_1, J_2 and J_3 are the Josephson currents flowing through each branch of the junction. (b) Basic star graph. L_j is the length of the j-th branch of the graph ($j = 1, 2, 3$).

detailed study of the problem using the sine-Gordon equation on networks in [26,27]. Some versions of Josephson junction networks containing chain of the linear superconductors connected via the point-like insulators have been studied on the basis of discrete sine-Gordon model [28–33]. Unlike the previously discussed versions of Josephson junction networks, our model is simple from the viewpoint of experimental realization and can be studied.

The paper is organized as follows. In the next section we give a formulation of the problem in terms of the sine-Gordon equation on metric graphs. The third section presents the derivation of exact analytical solutions for special cases and their stability analysis. Finally, the final section presents some concluding remarks.

Modeling of branched Josephson junction in terms of metric graph. – Consider the structure presented in fig. 1(a), which represents a Josephson junction consisting of three planar superconductors connected to each other via the branched insulator in the form of Y-junction. The whole system is assumed to interact with external constant magnetic field, H, which is perpendicular to the plane of superconductors. Such structure can be considered as the branched version of the Josephson junction considered in refs. [20,21]. The structure can be modeled in terms of metric star graph having three branches, *i.e.*, simple Y-junction (see, fig. 1(b)). For each bond of the star graph a coordinate x_j is assigned. The origin of coordinates at the vertex, 0 and for bonds we put $x_j \in [0; L_j]$. Then one can use shorthand notation $\phi_j(x)$ for $\phi_j(x_j)$, where x is the coordinate on the bond j to which the component ϕ_j refers. The phase difference on each branch ϕ_j, is described in terms of the stationary sine-Gordon equation on metric star graph [34]:

$$\frac{\mathrm{d}^2}{\mathrm{d}x^2}\phi_j = \frac{1}{\lambda_j^2}\sin(\phi_j), \quad 0 < x < L_j, \tag{1}$$

where $j = 1, 2, 3$ is the bond (branch) number and the origin of coordinates is assumed at the branching point, O. To solve this equation, one needs to impose boundary conditions at the branching point, O. Such boundary conditions can be derived from the physical properties of the structure presented in fig. 1(a). Computing, at the branching point, the phase differences, $\phi_1 = \theta_1 - \theta_3$, $\phi_2 = \theta_1 - \theta_2$, $\phi_3 = \theta_2 - \theta_3$, where $\theta_{1,2,3}$ are the phases on each superconductor, one can obtain first set of the vertex boundary conditions given by

$$\phi_1|_{x=0} - \phi_2|_{x=0} - \phi_3|_{x=0} = 0. \tag{2}$$

In the following we will use the system of units $\hbar = c = 2\pi d = e = 1$, where d is equal to twice the penetration depth (for identical superconductors) plus the insulator (or normal metal) thickness [54]. In such units, *e.g.*, for $d = 1\,\mathrm{mm}$ $J_j = 1$ is equal to $\approx 7.64\,\mathrm{nA}$, and for the magnetic field $H = 1$ implies that $H \approx 1.22\,\mu\mathrm{A/m}$, etc.

Then the local magnetic field in terms of ϕ_j can be written as

$$h_j(x) = \frac{\partial \phi_j}{\partial x}, \tag{3}$$

where we have scaled the local magnetic field over π (*i.e.*, $\frac{h_j(x)}{\pi} \to h_j(x)$). The current density on each branch of the junction is given as [21,54,55]

$$j_j(x) = \frac{1}{4\lambda_j^2}\sin\phi_j(x). \tag{4}$$

Integrating eq. (4) over the each bond and using eq. (1) we can find the current on each bond as [54]

$$J_j = \frac{1}{4}\left(\left.\frac{\mathrm{d}\phi_j}{\mathrm{d}x}\right|_{x=L_j} - \left.\frac{\mathrm{d}\phi_j}{\mathrm{d}x}\right|_{x=0}\right). \tag{5}$$

Using continuity of the local magnetic field $h_j(x)$ at the branching point ($h_1(0) = h_2(0) = h_3(0)$) we get the second set of vertex boundary conditions:

$$\left.\frac{\mathrm{d}\phi_1}{\mathrm{d}x}\right|_{x=0} = \left.\frac{\mathrm{d}\phi_2}{\mathrm{d}x}\right|_{x=0} = \left.\frac{\mathrm{d}\phi_3}{\mathrm{d}x}\right|_{x=0}. \tag{6}$$

For complete formulation of the problem, one needs also to impose boundary conditions at the end of each branch. This can be done by writing explicitly the value of local magnetic field in terms of external and intrinsic magnetic field. These latter are supposed to be induced by Josephson current on each branch. Denoting this magnetic field on each branch by H_{Jj} ($j = 1, 2, 3$) we have the following Neumann-type boundary conditions at the end of each branch:

$$\left.\frac{\mathrm{d}\phi_1}{\mathrm{d}x}\right|_{x=L_1} = H + H_{J1},$$
$$\left.\frac{\mathrm{d}\phi_2}{\mathrm{d}x}\right|_{x=L_2} = H - H_{J2},$$
$$\left.\frac{\mathrm{d}\phi_3}{\mathrm{d}x}\right|_{x=L_3} = H - H_{J3}. \qquad (7)$$

Writing the same expression at the branching point, one can derive explicit relation expressing the external magnetic field, H in terms of the derivatives of phase differences:

$$H = \frac{1}{4}\sum_{j=1}^{3}\left.\frac{\mathrm{d}\phi_j}{\mathrm{d}x}\right|_{x=L_j} + \frac{1}{4}\left.\frac{\mathrm{d}\phi_1}{\mathrm{d}x}\right|_{x=0}. \qquad (8)$$

The problem given by eqs. (1), (2), (6) and (7) completely determines the problem of sine-Gordon equation on metric star graph, which is the model for the static solitons in the branched Josephson junction presented in fig. 1(a).

Exact solutions of eq. (1) for the boundary conditions providing the absence of current-carrying states ($J_j = 0$), have been obtained in [34], where the stability of such solutions also was analyzed. Here we consider current-carrying states ($J_j \neq 0$) in the branched Josephson junction, which are described by different boundary conditions.

Static solitons and their stability. – The problem given by eqs. (1), (2), (6) and (7) have different types of solutions. However, only the stable solutions of this problem can be considered as the physical ones. These latter describe the phase difference in branched Josephson junction in fig. 1(a). Therefore, following refs. [20,21], we provide prescription for stability analysis for the solutions of eq. (1). Starting point for such analysis is the Gibbs free-energy functional which can be written as [20,21]

$$\Omega_G = \sum\nolimits_{j=1}^{3}\Omega_G^{(j)}\left[\phi_j, \frac{\mathrm{d}\phi_j}{\mathrm{d}x}; H, H_{J1}, H_{J2}, H_{J3}\right], \qquad (9)$$

where $\Omega_G^{(j)}$ is the Gibbs free energy functional on each bond (see ref. [23] for details of the derivation of Ω_G), which is given by

$$\Omega_G^{(j)}\left[\phi_j, \frac{\mathrm{d}\phi_j}{\mathrm{d}x}; H, H_{J1}, H_{J2}, H_{J3}\right] = 2H^2 L_j$$
$$-\left(H \pm H_{Jj}\right)\phi_j(L_j)$$
$$+\left(H - H_{J1} + H_{J2} + H_{J3}\right)\phi_j(0)$$
$$+\int_0^{L_j}\left[\frac{1}{\lambda_j^2}\left(1-\cos\phi_j(x)\right) + \frac{1}{2}\left(\frac{\mathrm{d}\phi_j(x)}{\mathrm{d}x}\right)^2\right]\mathrm{d}x, \qquad (10)$$

where we take the "+" sign for $j = 1$, and "−" sign for other cases. Equation (1) together with the boundary conditions (2), (6), (7) follows from the condition

$$\delta\Omega_G = 0. \qquad (11)$$

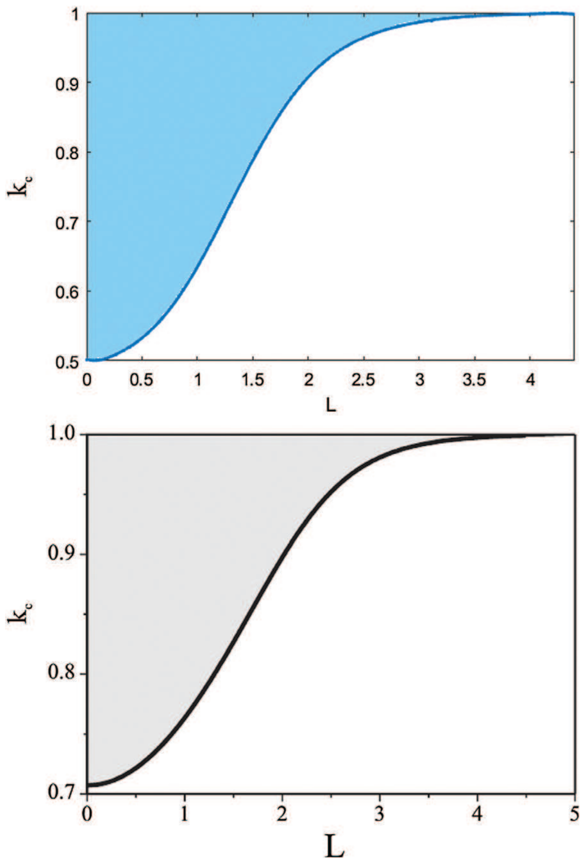

Fig. 2: Upper panel: The dependence of the stability border, $k_c = k_c(L)$ on the branch length (solid line) for the branched Josephson junction. The colored area corresponds to the stability area. Lower panel: similar plot in the linear (unbranched) case from ref. [21].

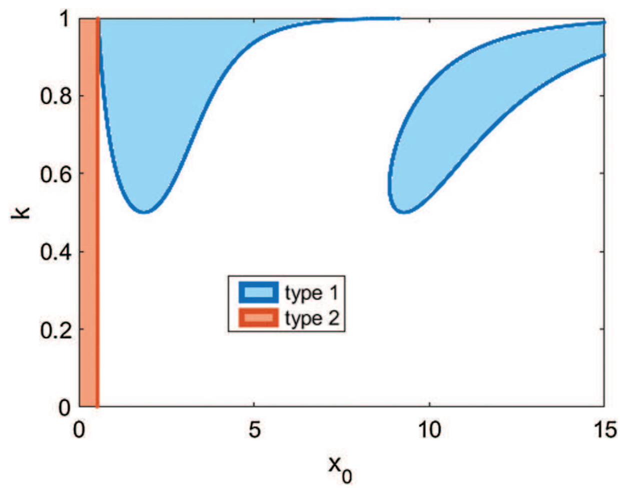

Fig. 3: The stability region (colored) of ϕ in the parametric plane. Branch lengthes are $L_1 = 1, L_2 = 2, L_3 = 3$.

The criterion for the stability of the solution of the problem given by eqs. (1), (2), (6) and (7), can be obtained from the second variation of Ω_G, which leads to

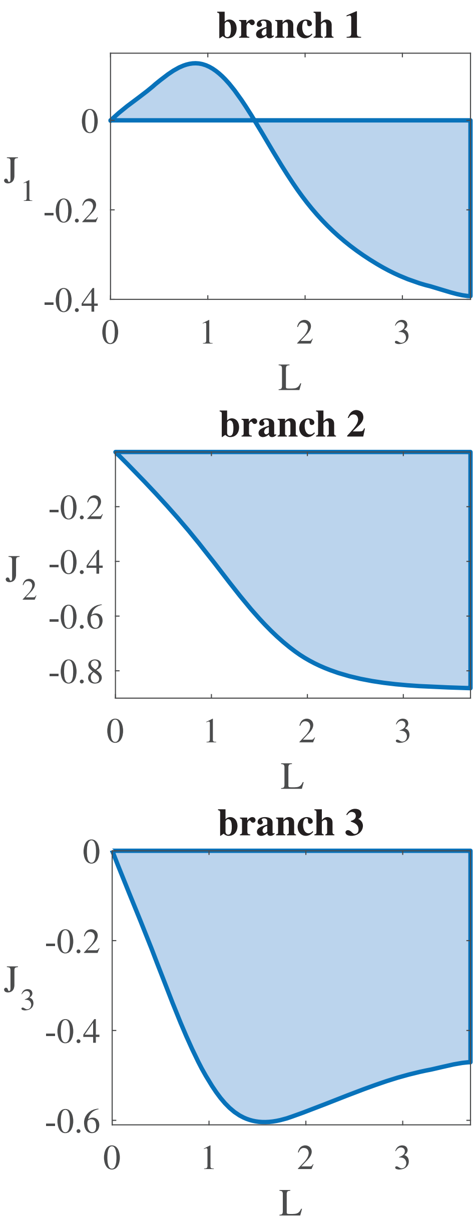

Fig. 4: The dependence $J_c = J_c(L)$ for $H = 0$ (solid line). The stability region is colored, parameters are the same as in fig. 2.

the following Sturm-Liouville problem [20,21,34]:

$$
\begin{aligned}
&-\frac{\mathrm{d}^2\psi_j}{\mathrm{d}x^2} + \frac{1}{\lambda_j^2}\cos\phi_j(x)\psi_j = \mu\psi_j, \quad 0 < x < L_j, \\
&\psi_1|_{x=0} - \psi_2|_{x=0} - \psi_3|_{x=0} = 0, \\
&\left.\frac{\mathrm{d}\psi_1}{\mathrm{d}x}\right|_{x=0} = \left.\frac{\mathrm{d}\psi_2}{\mathrm{d}x}\right|_{x=0} = \left.\frac{\mathrm{d}\psi_3}{\mathrm{d}x}\right|_{x=0}, \\
&\left.\frac{\mathrm{d}\psi_j}{\mathrm{d}x}\right|_{x=L_j} = 0, \qquad j = 1, 2, 3,
\end{aligned} \tag{12}
$$

where $\psi_j = \delta\phi_j$, $j = 1, 2, 3$. In terms of the lowest eigenvalue, μ_0, the criterion for stability of the solution can be formulated as follows. If $\mu_0 < 0$, the solution $\phi_j(x)$ corresponds to a saddle point of eq. (9) which implies that the solution is absolutely unstable and unphysical. Stable (physical) solutions correspond to the case, when $\mu_0 > 0$, ($\delta^2\Omega_G > 0$). The boundaries of the stability regions for these solutions is determined by the condition $\mu_0 = 0$ ($\delta^2\Omega_G = 0$), that leads to the following Sturm-Liouville problem:

$$
-\frac{\mathrm{d}^2\bar{\psi}_j}{\mathrm{d}x^2} + \frac{1}{\lambda_j^2}\cos\phi_j(x)\bar{\psi}_j = 0, \quad 0 < x < L_j, \tag{13}
$$

$$
\bar{\psi}_1|_{x=0} - \bar{\psi}_2|_{x=0} - \bar{\psi}_3|_{x=0} = 0, \tag{14}
$$

$$
\left.\frac{\mathrm{d}\bar{\psi}_1}{\mathrm{d}x}\right|_{x=0} = \left.\frac{\mathrm{d}\bar{\psi}_2}{\mathrm{d}x}\right|_{x=0} = \left.\frac{\mathrm{d}\bar{\psi}_3}{\mathrm{d}x}\right|_{x=0}, \tag{15}
$$

$$
\left.\frac{\mathrm{d}\bar{\psi}_j}{\mathrm{d}x}\right|_{x=L_j} = 0, \qquad j = 1, 2, 3. \tag{16}
$$

Using eqs. (13)–(16), one can explicitly find the stability boundary for each type of solution of the problem given by eqs. (1), (2), (6) and (7).

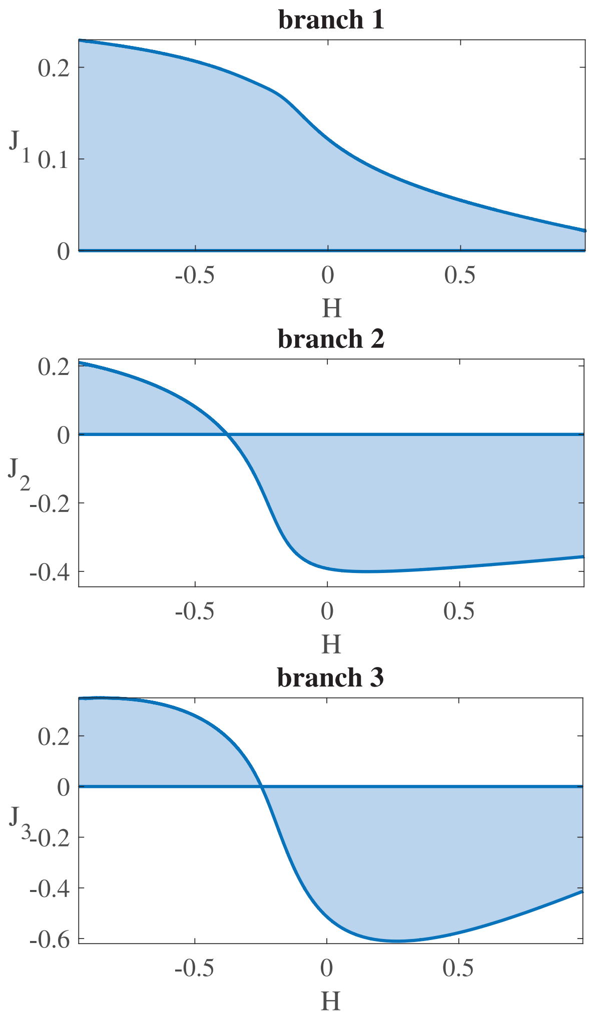

Fig. 5: The stability region (colored) of ϕ_j in the physical plane (J, H) for type I solutions and the same parameters as in fig. 3.

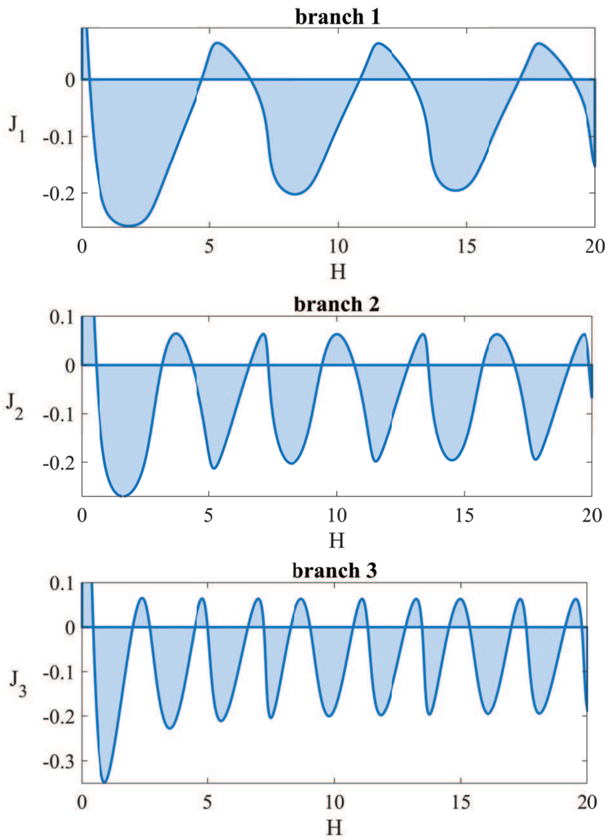

Fig. 6: The stability region (colored) of ϕ_j in the physical plane (J, H) for type II solutions and the same parameters as in fig. 3.

The general solution of eq. (1) can be obtained from the following first integral [20,21]:

$$\frac{1}{2}\left[\frac{\mathrm{d}\phi_j}{\mathrm{d}x}\right]^2 + \cos\phi_j = C_j, \quad -1 \le C_j < \infty, \tag{17}$$

with C_j being the integration constant. Depending on the value of C_j this general solution can be determined as type I and II. Namely, for $C_j \in [-1, 1)$ we have solution of type I, while solution of type II corresponds to the values, $C_j \in [1, \infty)$. Both solutions for $H \neq 0$, and $J_j = 0$ have been found in [47] where it was shown that only the special case of the solution of type II is stable. following refs. [20,21], instead of C_j we introduce new parametrization constant, k_j, which is defined, for the solution of type I as

$$k_j^2 \equiv \frac{1 + C_j}{2}, \qquad -1 < k_j < 1$$

and

$$k_j^2 \equiv \frac{2}{1 + C_j}, \qquad -1 < k_j < 1,$$

for the solution of type II. The general (type I) solution of eq. (1) can be written as [20,21,34]

$$\phi_j(x) = (2n_j + 1)\pi + 2\arcsin\left\{k_j sn\left[\frac{x - x_{0j}}{\lambda_j}, k_j\right]\right\} \tag{18}$$

where sn is the Jacobi elliptic function [56], and x_{0j} are integration constants which obey the constraints given by the following inequality:

$$-\lambda_j K(k_j) < x_{0j} < \lambda_j K(k_j), \quad j = 1, 2, 3.$$

The solution given by eq. (18) fulfils the vertex boundary conditions given by eqs. (2), (6) and (7), *i.e.*, it becomes the exact analytical solution of the problem given by eqs. (1), (2), (6) and (7), provided the following constraints hold true:

$$\lambda_1 = \lambda_2 = \lambda_3 = \lambda, \qquad k_1 = k_2 = k_3 = k,$$

$$-\frac{x_{01}}{\lambda_1} = \frac{x_{02}}{\lambda_2} = \frac{x_{03}}{\lambda_3} = x_0. \tag{19}$$

$$n_1 = n_2 + n_3. \tag{20}$$

Solution (18) can be stable only for those values of k which belong to the interval $[k_c, 1)$ ($k_c sn[x_0, k_c] = \frac{1}{2}$). Therefore in the following, in analogy with that in ref. [21], we compute the physical characteristics of the system at $k = k_c(x_0)$ which correspond to its values at the stability border. Using the relation

$$\frac{\mathrm{d}\phi_j(x)}{\mathrm{d}x} = -\frac{2k}{\lambda} cn\left[\frac{x}{\lambda} \pm x_0, k\right], \tag{21}$$

and eq. (7), when $j = 1$ we take $+$ sign, when $j = 2, 3$ we take $-$ sign, the stability border for the current-carrying states can be written as

$$J_j^{(c)} = -\frac{k_c}{2\lambda}\left(cn\left[\frac{L_j}{\lambda} \pm x_0, k_c\right] - cn\left[x_0, k_c\right]\right), \tag{22}$$

$$H^{(c)} = -\frac{k_c}{2\lambda}\left(\sum_{j=1}^{3} cn\left[\frac{L_j}{\lambda} \pm x_0, k_c\right] + cn\left[x_0, k_c\right]\right). \tag{23}$$

Figure 2 presents plot of k_c as a function of the parameter, L determined from $L_1 = L, L_2 = 2L, L_3 = 3L$. The left (colored) area of each plot corresponds to the stability region. Lower panel in this figure presents corresponding plot for linear case from ref. [21]. Since k_c appears as the value of k at which the Sturm-Liouville (stability) problem has zero ($\mu_0 = 0$) eigenvalue, it is important to check at which values of x_0 this is possible. Figure 3 presents plot of k_c as a function of x_0, *i.e.*, the stability region of ϕ in the parametric plane. The colored area corresponds to the stability region.

The solution of type II can be treated similarly to that of type I, by considering two cases. The case $H > 0$, $J_j = 0$ has been studied in detail in ref. [34]. Therefore we drop this part. Here we will focus on the case $H > 0$, $J_j > 0$. The general (type II) solution for this case can be written as

$$\phi_j(x) = \pi(2n_j + 1) + 2am\left(\frac{x - x_{0j}}{\lambda_j k_j}, k_j\right). \tag{24}$$

Fulfilling the boundary conditions given by eqs. (2) and (6) leads to the constraints in eqs. (19) and (20). Stable solutions and the border between stability and unstable

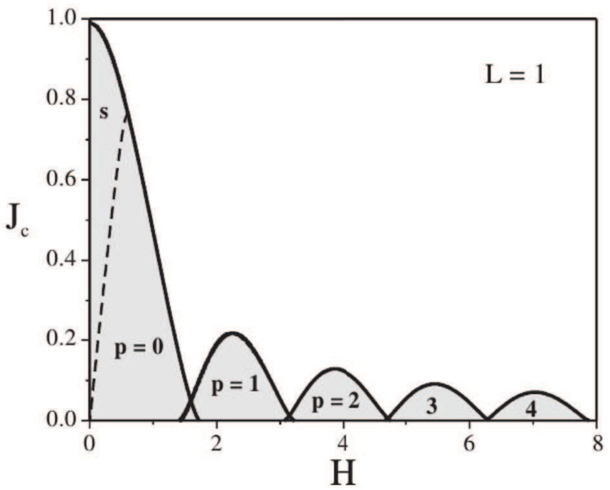

Fig. 7: The stability region of ϕ_j in the physical plane (J, H) for the linear (unbranched) Josephson junction from ref. [21].

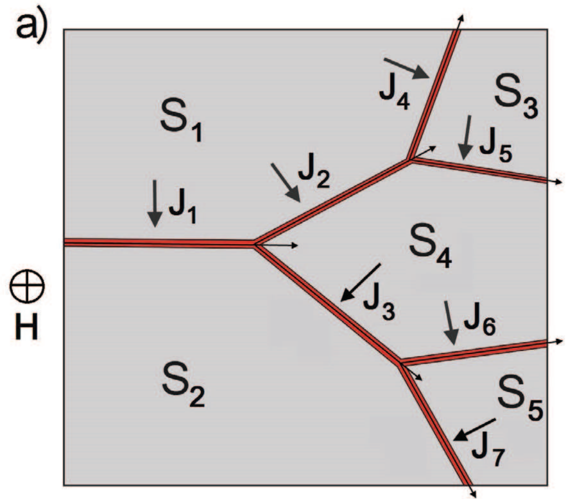

Fig. 8: Tree-like branched Josephson junction.

regions can be determined similarly to that for solution type I.

From eqs. (5) and (8) we get the expressions for current and magnetic field:

$$J_j = \frac{1}{2\lambda k}\left(dn\left[\frac{L_j}{\lambda k} \pm x_0, k\right] - dn\left[x_0, k\right]\right), \qquad (25)$$

$$H = \frac{1}{2\lambda k}\left(\sum_{j=1}^{3} dn\left[\frac{L_j}{\lambda k} \pm x_0, k\right] + dn\left[x_0, k\right]\right), \qquad (26)$$

$$x_0 \in [0; x_{0,c}]. \qquad (27)$$

In fig. 4, the dependence of the current on the branch length, L_j is plotted. Colored (lower) parts corresponds to the the stability area. Figures 5 and 6 present the plots of the current, J_j as a function of the magnetic field for type I and type II, respectively. The colored area in each plot corresponds to the stability region, *i.e.*, presents the stability region of ϕ_j in the physical plane (J, H).

It is meaningful to compare the above results with those for their linear (unbranched) counterpart considered in ref. [21]. Comparing dependence of k_c on L presented in fig. 2 with the corresponding plot for the linear case, one can conclude that they are very close to each other. However, differences between linear and branched cases appear in the plots of $J_j(L)$ and $J_j(H)$ presented in figs. 3–6, respectively. Comparing $J_j(H)$ in figs. 5 and 6 for the branched Josephson junction with the corresponding plot in fig. 7 for the linear case, one can find considerable difference both in the shape and area of the stability region. In particular, for the branched case the total area of the stability region is much larger than that for the linear counterpart. Moreover, due to the fact that the branched system has more parameters, one can make it tunable with respect to playing with these parameters. Especially, this concerns the case of more complicated branching architecture, *e.g.*, junction with tree-like branching presented in fig. 8. Static solitons in this structure can be modeled in terms of the sine-Gordon equation with the boundary conditions given on metric tree graph.

Conclusions. – We have studied the current-carrying states in the branched Josephson junction interacting with the external magnetic field. The structure is assumed to be constructed, from three planar superconductors connected to each other via the insulating (or normal metal) Y-junction. The system is modeled in terms of the stationary sine-Gordon equation on the metric star graph, whose solutions describe the phase difference between the superconductors on the each branch of the junction. The boundary conditions for the sine-Gordon equation at the branching point are derived from the relation between current, local and external magnetic fields. Exact analytical solutions of the sine-Gordon equation fulfilling such boundary conditions are obtained. The stability regions for these solutions are determined in terms of the integration constant using the Gibbs free energy functional based (variational) approach. Physical observable values of the current described in terms of the stable solutions are derived explicitly as a function of the magnetic field. Finally, we note that although we considered very simple branching having the form of Y-junction, the approach we used can be directly extended for modeling static solitons in more general branching architectures of the junction, such as tree, loop, triangle, etc. This can be done similarly to [34], where the sine-Gordon equation on metric graphs is solved for $J_j = 0$. Considering such complicated branching architectures is of importance from the viewpoint of the device tuning and optimization in such problems as SQUID, superconducting qubit, cold atom trapping and Majorana wire networks.

* * *

This work is supported by the grant of the Ministry for Innovation Development of Uzbekistan (Ref. No. BF2-022).

REFERENCES

[1] Josephson B. D., *Rev. Mod. Phys.*, **36** (1964) 216.
[2] Josephson B. D., *Rev. Mod. Phys.*, **46** (1974) 251.
[3] Barone A. and Paterno G., *Physics and Applications of the Josephson Effect* (Wiley, New York) 1982.
[4] Likharev K. K., *Dynamics of Josephson Junctions and Circuits* (CRC Press) 1986.
[5] McCann J., *Josephson Junction and Superconductivity Research* (Nova Science Publishers) 2007.
[6] Wolf E. L., Arnold G. B., Gurvitch M. A. and Zasadzinski J. F. (Editors), *Josephson Junctions: History, Devices, and Applications* (Pan Stanford Publishing) 2017.
[7] Askerzade I., Bozbey A. and Canturk M., *Modern Aspects of Josephson Dynamics and Superconductivity Electronics* (Springer) 2017.
[8] Cuevas-Maraver J., Kevrekidis P. G. and Williams F. (Editors), *The Sine-Gordon Model and Its Applications: From Pendula and Josephson Junctions to Gravity and High-Energy Physics* (Springer International Publishing) 2014.
[9] Ablowitz M. J. and Segur H., *Solitons and the Inverse Scattering Transform* (SIAM, Philadelphia) 1981.
[10] Rajaraman R., *Solitons and Instantons* (Elsevier, Amsterdam) 1982.
[11] Drazin P. G. and Johnson R. S., *Solitons: An Introduction* (Cambridge University Press) 1989.
[12] Ablowitz M. J. and Clarkson P. A., *Solitons, Nonlinear Evolution Equations and Inverse Scattering* (Cambridge University Press) 1999.
[13] Dauxois T. and Peyrard M., *Physics of Solitons* (Cambridge University Press, Cambridge) 2006.
[14] Scott A. C., *Nonlinear Science, Emergence and Dynamics of Coherent Structures* (Oxford University Press) 2003.
[15] Braun O. and Kivshar Yu., *The Frenkel-Kontorov Model* (Springer) 2004.
[16] Malomed B. A., *Phys. Rev. B*, **39** (1989) 8018(R).
[17] Ustinov A. V., Doderer T., Huebener R. P. *et al.*, *Phys. Rev. Lett*, **69** (1992) 1815.
[18] Hermon Z., Ben-Jacob E. and Schoen G., *Phys. Rev. B*, **54** (1996) 1234.
[19] Carapella G., Costabile G. and Sabatino P., *Phys. Rev. B*, **58** (1998) 15094.
[20] Kuplevakhsky S. V. and Glukhov A. M., *Phys. Rev. B*, **73** (2006) 024513.
[21] Kuplevakhsky S. V. and Glukhov A. M., *Phys. Rev. B*, **76** (2007) 174515.
[22] Fedorov K. G., Fistul M. V. and Ustinov A. V., *Phys. Rev. B*, **84** (2011) 014526.
[23] Kuplevakhsky S. V., *Low Temp. Phys.*, **30** (2004) 646.
[24] Nakajima K., Onodera Y. and Ogawa Y., *J. Appl. Phys.*, **49** (1978) 2958.
[25] Kogan V., Clem J. and Kirtley J., *Phys. Rev. B*, **61** (2000) 9122.
[26] Susanto H., van Gils S., Doelman A. and Derks G., *Physica C*, **408** (2004) 579.
[27] Susanto H., van Gils S., Doelman A. and Derks G., *Phys. Rev. B*, **69** (2004) 212503.
[28] De Luca R. and Romeo F., *Phys. Rev. B*, **66** (2002) 024509.
[29] Giuliano D. and Sodano P., *EPL*, **88** (2009) 17012.
[30] Giuliano D. and Sodano P., *Nucl. Phys. B*, **811** (2009) (FS) 395.
[31] Giuliano D. and Sodano P., *Nucl. Phys. B*, **837** (2010) (FS) 153.
[32] Giuliano D. and Sodano P., *EPL*, **103** (2013) 57006.
[33] Ovchinnikov Yu. N. and Kresin V. Z., *Phys. Rev. B*, **88** (2013) 214504.
[34] Sabirov K. K., Rakhmanov S., Matrasulov D. and Susanto H., *Phys. Lett. A*, **382** (2018) 1092.
[35] Sobirov Z., Matrasulov D., Sabirov K., Sawada S. and Nakamura K., *Phys. Rev. E*, **81** (2010) 066602.
[36] Sobirov Z., Matrasulov D., Sawada S. and Nakamura K., *Phys. Rev. E*, **84** (2011) 026609.
[37] Adami R., Cacciapuoti C., Finco D. and Noja D., *Rev. Math. Phys.*, **23** (2011) 4.
[38] Sabirov K. K., Sobirov Z. A., Babajanov D. and Matrasulov D. U., *Phys. Lett. A*, **377** (2013) 860.
[39] Noja D., *Philos. Trans. R. Soc. A*, **372** (2014) 20130002.
[40] Caputo J.-G. and Dutykh D., *Phys. Rev. E*, **90** (2014) 022912.
[41] Uecker H., Grieser D., Sobirov Z., Babajanov D. and Matrasulov D., *Phys. Rev. E*, **91** (2015) 023209.
[42] Noja D., Pelinovsky D. and Shaikhova G., *Nonlinearity*, **28** (2015) 2343.
[43] Adami R., Cacciapuoti C. and Noja D., *J. Differ. Equ.*, **260** (2016) 7397.
[44] Caudrelier V., *Commun. Math. Phys.*, **338** (2015) 893.
[45] Sobirov Z., Babajanov D., Matrasulov D., Nakamura K. and Uecker H., *EPL*, **115** (2016) 50002.
[46] Adami R., Serra E. and Tilli P., *Commun. Math. Phys.*, **352** (2017) 387.
[47] Kairzhan A. and Pelinovsky D. E., *J. Phys. A: Math. Theor.*, **51** (2018) 095203.
[48] Bolte J. and Harrison J., *J. Phys. A: Math. Gen.*, **36** (2003) L433.
[49] Sabirov K. K., Yusupov J., Jumanazarov D. and Matrasulov D., *Phys. Lett. A*, **382** (2018) 2856.
[50] Sabirov K. K., Babajanov D. B., Matrasulov D. U. and Kevrekidis P. G., *J. Phys. A: Math. Theor.*, **51** (2018) 435203.
[51] Yusupov J. R., Sabirov K. K., Ehrhardt M. and Matrasulov D. U., *Phys. Lett. A*, **383** (2019) 2382.
[52] Babajanov D., Matyoqubov H. and Matrasulov D., *J. Chem. Phys.*, **149** (2018) 164908.
[53] Yusupov J. R., Sabirov K. K., Ehrhardt M. and Matrasulov D. U., *Phys. Rev. E*, **100** (2019) 032204.
[54] Owen C. S. and Scalapino D. J., *Phys. Rev.*, **164** (1967) 538.
[55] Zharkov G. F., *Sov. Phys. JETP*, **48** (1970) 1107.
[56] Abramowitz M. and Stegun I. A., *Handbook of Mathematical Functions* (Dover, New York) 1965.